Graphitic Carbon Nitride/TiO_2 Heterostructures for Photocatalytic Hydrogen Evolution

Eric Thornburg Literature Seminar October 25, 2018

At current rates of population growth and industrialization, the US Energy Information Administration estimates that world energy consumption will increase 48% by 2040.[1] As this occurs, it will be vital that humans shift away from the burning of fossil fuels, due to both limited natural reserves and the harsh environmental effects of their collection, processing, and use. One potential form of renewable energy is molecular hydrogen, which carries almost three times the specific energy (MJ/m^3) of liquid fossil fuels.[2] The combustion of hydrogen fuel with oxygen yields only water, making it an ideal clean energy source as well. Despite this, modern industrial-scale production of hydrogen is mostly achieved by way of steam reforming, a process that involves abstracting hydrogen from fossil fuels at high pressures and temperatures (13-20 bar and 800-1000°C).[2] For hydrogen fuel to become a feasible source of clean energy, new production methods that do not rely on fossil fuels and are much less energy-intensive must be developed.

Since the seminal work of Fujishima and Honda on the photoelectrochemical splitting of water using TiO_2 electrodes, semiconductor-mediated photocatalysis has shown great promise as a means for the renewable production of hydrogen from electromagnetic energy.[3] Most recent research is directed toward nano- or mesoscale semiconductor particles and heterostructures, which Bard showed could function as stand-alone photo(electro)catalytic systems in solution.[4] These particulate systems have the benefits of greater specific surface area as well as more efficient light absorption while suspended. In general, the photocatalytic mechanism includes three steps: (1) absorption of light with energy higher than or equal to the semiconductor's band gap, creating electron-hole pairs; (2) separation and migration of electrons and holes to surface sites; and (3) concomitant reduction and oxidation of species adsorbed to the catalyst by the electrons and holes, respectively.[5] Thus in order to maximize efficiency, any given photocatalyst should have high light absorption, high specific surface area, quick and long-lived separation of charges, and, for hydrogen evolution, a band gap larger than the free energy change necessary to split water (1.23 eV).[6] A general schematic diagram of a water-splitting photocatalyst is displayed in Fig. 1.

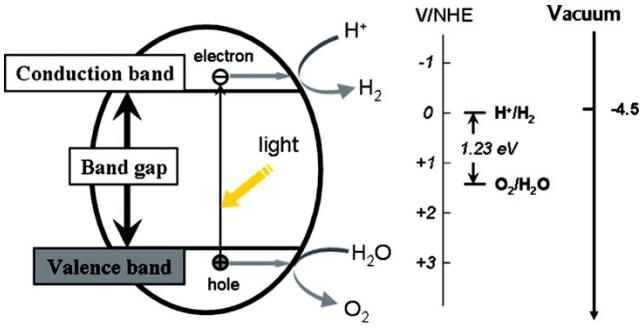

Figure 1. Schematic diagram of a particulate photocatalyst for overall water splitting. In the examples below, a sacrificial agent is oxidized. Adapted from Ref. 6.

Although the past few decades of research have yielded numerous novel materials for photocatalytic hydrogen evolution, many of those published have been based on semiconducting metal oxides.[6,7] These materials (*e.g.* TiO_2, $SrTiO_3$ ZnO) can achieve apparent quantum efficiencies of up to 30% and hydrogen evolutions rates of ~6500 μmol $h^{-1}g^{-1}$ with the aid of Pt/RuO_2 or Rh cocatalysts, but often have band gaps larger than 3.0 eV, meaning they will only absorb UV radiation (ca. 4% of solar radiation). Other examples of semiconducting sulfides, doped semiconductors, and complex solid solutions used for photocatalytic hydrogen evolution are capable of absorbing visible light, but often exhibit unfavorable photoinduced degradation or require complicated synthetic procedures and the use of rare and/or toxic elements.[6,7]

The use of graphitic carbon nitride (g-C_3N_4) in photocatalytic heterostructures is a convenient way around many of these limitations. While carbon nitride can exist as multiple different allotropes, the most stable form in ambient conditions is the sp^2 hybridized graphite analogue. Originally discovered as early as 1834 by Berzelius and Liebig in the embryonic form of "melon"—a linear-chain polymer consisting of repeating tri-*s*-triazine units (also called melem, see Fig. 2) —the structure of bulk g-C_3N_4 was not fully understood until almost 100 years later.[8,9]

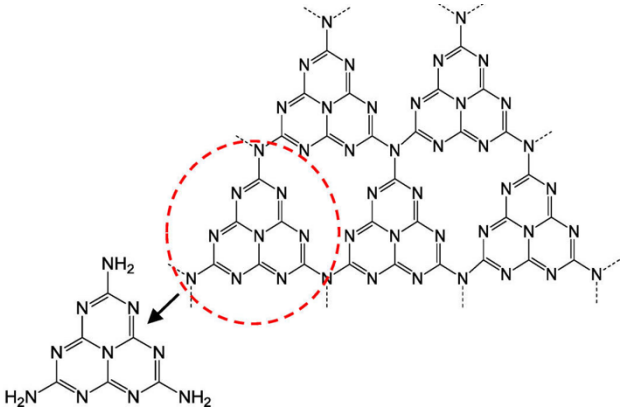

Figure 2. Structure of the 2D planes in g-C_3N_4. The repeating unit, melem, is shown bottom left.

It is now known that g-C_3N_4 is composed of 2D sheets of tri-*s*-triazine units (C_6N_7) linked at tertiary amines (Fig. 2). Bulk g-C_3N_4 powder is nontoxic and can be easily synthesized by thermal polycondensation of cheap, nitrogen-rich precursors such as cyanamide, dicyandiamide, melamine, thiourea, or urea.[9,10] Owing to its graphitic structure, g-C_3N_4 is also thermally stable up to 600°C and chemically stable in organic solvents as well as in acidic and alkaline solution.[8,9] Importantly, the moderate band gap of g-C_3N_4 (2.7 eV) allows visible light absorption at wavelengths below 460 nm, and the conduction and valence bands of g-C_3N_4 sit at roughly -1.1 eV and +1.6 eV versus the normal hydrogen electrode, respectively.[5,8-11]

In 2009, Wang et al. reported visible light-driven photocatalytic hydrogen evolution over g-C_3N_4 for the first time.[11] Using pristine g-C_3N_4 powder and triethanolamine as a sacrificial electron donor in water, hydrogen could be evolved at rates of up to 4 μmol h^{-1}. When loaded with 3 wt% Pt cocatalyst, this activity increased seven-fold, due to increased charge separation and reduced activation energy of H-H bond formation at the Pt surface.[11] The publication of this paper caused an explosion of interest in g-C_3N_4 for photocatalytic applications, due to its ability to utilize a larger portion of the solar spectrum for photocatalytic hydrogen evolution than many previous photocatalysts. It also became clear that to optimize g-C_3N_4 for photocatalysis, the formation of herterostructures with other semiconducting materials should be pursued. The goal of this would be to impart more efficient charge carrier separation in g-C_3N_4 and increase specific surface areas, thus increasing the number of available adsorption sites on the catalyst.[5,8,9] The remainder of this discussion will center about the engineering of g-C_3N_4/TiO_2 heterostructures for these purposes.

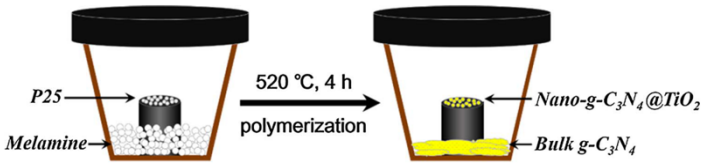

Figure 3. Synthesis of nano-g-C_3N_4/TiO_2 by a facile vapor deposition method. Adapted from Ref. 12.

One recent study by Tan and coworkers achieved greatly enhanced photocatalytic hydrogen evolution by the facile nanostructuring of g-C_3N_4 on commercial TiO_2 supports.[12] While previous reports of nanostructured g-C_3N_4/TiO_2 involve complex multistep synthetic procedures, the authors of this paper use a one-step vapor deposition method (Fig. 3). The obtained heterostructures were characterized by XRD, FT-IR, TEM, and XPS to confirm formation of the g-C_3N_4 composite. Slight shifts in the XRD peaks for nanostructured g-C_3N_4 as compared to bulk

g-C_3N_4 indicated closer interlayer spacing and increased planarization of layers due to the nanostructuring, while peaks from TiO_2 remain undisturbed. Diffuse reflectance absorbance spectroscopy indicated good light absorption at wavelengths below 450 nm, and specific surface areas of the heterostructures were augmented by a factor of 7 over bulk g-C_3N_4. Photoluminescence spectra of the composites indicated greatly improved charge carrier separation, and characterization of photocatalytic hydrogen production in the presence of small concentrations of Pt cocatalyst (3 wt%) and triethanolamine sacrificial agent found evolution rates of 513 µmol $h^{-1}g^{-1}$. The reported apparent quantum efficiency (AQE) was also 0.31% under 420 nm light. This is quite low, although it should be noted that the equation used to calculate this was actually closer to that used in calculating overall solar to hydrogen efficiency, meaning AQE is likely higher.

Another very recent report by Yu et al. also works toward optimizing g-C_3N_4/TiO_2 heterostructures.[13] In this case, bulk polymerized g-C_3N_4 was ground and combined with titanium tetrachloride. The mixture was dispersed in acetone, ultrasonicated, and sealed in an autoclave to be heated at 125°C for 24 hours (Fig. 4). Mesoporous TiO_2 self-doped with Ti^{3+} formed heterostructured composites with the g-C_3N_4, and these were characterized by similar suite of methods as in the previous study to confirm the structures. Specifically, XPS spectra confirmed the presence of Ti^{3+} in the composites. Additionally, slight decrease in the binding energies of Ti-2*p* electrons in these spectra indicated the formation of new chemical bonds in the heterostructures as compared to pristine Ti^{3+} doped mesocrystalline TiO_2. Appreciable light absorption by the heterostructures also began at wavelengths lower than 450 nm, and specific surface areas were almost 25 times higher than that of bulk-C_3N_4. Photoluminescence and time-resolved fluorescence spectra of the composites indicated greatly increased charge carrier lifetimes, and photocatalytic hydrogen production in the presence of 1 wt% Pt cocatalyst and triethanolamine sacrificial agent yielded evolution rates of 3748 µmol $h^{-1}g^{-1}$ with AQE of 1.42% at wavelengths above 400 nm.

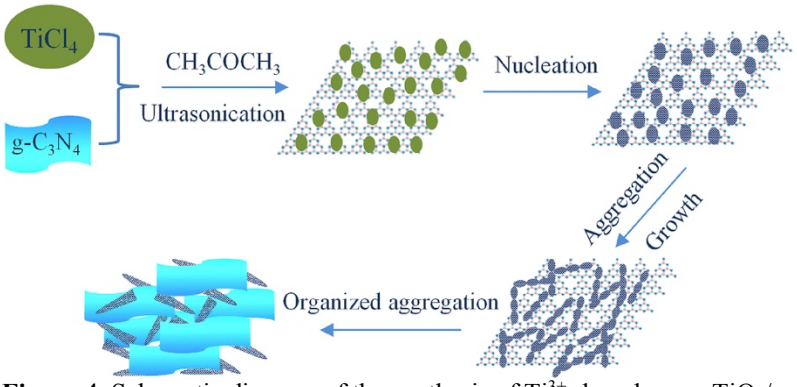

Figure 4. Schematic diagram of the synthesis of Ti^{3+}-doped meso-TiO_2/g-C_3N_4 heterostructures. Adapted from Ref. 13.

The authors of these two studies suggest different mechanisms for photocatalytic enhancement in the two systems. While heterostructures in the latter study performed better for hydrogen evolution, more characterization, perhaps by time-resolved optical and X-ray methods, needs to be completed on similar systems to confirm mechanistic details.[5] Overall, though, g-C_3N_4/TiO_2 heterostructures show great promise for applications in photocatalytic hydrogen evolution, due to their facile construction from earth-abundant elements, low toxicity, high stability, and visible-light absorption. However, efforts should be made to enhance quantum efficiencies of these structures and couple hydrogen production to oxygen evolution for overall water splitting.

References

1. *International Energy Outlook 2018.* US Energy Information Administration, **2018**.
2. Hosseini, S.E.; Wahid, M.A. *Renewable and Sustainable Energy Reviews* **2016**, *57*, 850-866.
3. Fujishima, A.; Honda, K. *Nature* **1972**, *238*, 37-38.
4. Bard, A.J. *Journal of Photochemistry* **1979**, *10*, 59-75.
5. Fu, J.; Yu, J.; Jiang, C.; Cheng, B. *Adv. Energy Mat.* **2018**, *8*, 1701503.
6. Chen, X.; Shen, S.; Guo, L.; Mao, S.S. *Chem. Rev.* **2010**, *110*, 6503-6570.
7. Chen, S.; Takata, T.; Domen, K. *Nat. Rev. Mater.* **2017**, *2*, 17050.
8. Ong, W.J.; Tan, L.L.; Ng, Y.H.; Yong, S.T.; Chai, S.P. *Chem. Rev.* **2016**, *116*, 7159-7329.
9. Cao, S; Low, J.; Yu, J.; Jaroniec, M. *Adv. Mat.* **2015**, *27*, 2150-2176.
10. Thomas, A; Fischer, A; Goettmann, F.; Antionetti, M.; Mueller, J.O.; Schloegl, R; Carlsson, J.M. *J. Mater. Chem.* **2008**, *18*, 4893-4908.
11. Wang, X.; Maeda, K.; Thomas, A.; Takanabe, K.; Xin, G.; Carlsson, J.M.; Domen, K.; Antionetti, M. *Nat. Mater.* **2009**, *8*, 76-80.
12. Tan, Y.; Shu, Z.; Zhou, J.; Li, T.; Wang, W.; Zhao, Z. *Appl. Catal. B: Eviron.* **2018**, *230*, 260-268.
13. Yu, X.; Fan, X.; An, L.; Liu, G.; Li, Z.; Liu, J.; Hu, P. *Carbon* **2018**, *128*, 21-30.